HHS Public Access

Author manuscript

Chem Res Toxicol. Author manuscript; available in PMC 2019 May 13.

Published in final edited form as:

Chem Res Toxicol. 2018 September 17; 31(9): 985–990. doi:10.1021/acs.chemrestox.8b00178.

Gas/Particle Partitioning Constants of Nicotine, Selected Toxicants, and Flavor Chemicals in Solutions of 50/50 Propylene Glycol/Glycerol As Used in Electronic Cigarettes

James F. Pankow[*,†,‡], **Kilsun Kim**[†], **Wentai Luo**[†,‡], and **Kevin J. McWhirter**[†,‡]

[†]Department of Chemistry, Portland State University, Portland, Oregon 97229, United States

[‡]Department of Civil and Environmental Engineering, Portland State University, Portland, Oregon 97229, United States

Abstract

For an electronic cigarette (e-cigarette) aerosol with known total particulate matter concentration (TPM, $\mu g/m^3$), predictions of the fractions of some compound i in the gas and particle phases ($f_{g,i}$ and $f_{p,i}$) at equilibrium can be made based on $K_{p,i}$ ($m^3/\mu g$), the compound-dependent gas/particle partitioning equilibrium constant. $f_{g,i}$ and $f_{p,i}$ affect the modes and locations of deposition in the respiratory tract. $K_{p,i}$ depends inversely on (1) the pure compound liquid vapor pressure ($p^o_{L,i}$), (2) mole fraction activity coefficient (ζ_i) in the absorbing liquid, and (3) mean molecular weight of the absorbing liquid ($\overline{MW}$). $K_{p,i}$ values were measured at 20 °C for 32 compounds as spiked into simulated e-cigarette liquids prepared as 50/50 mixtures (by weight) of propylene glycol (PG) and glycerol (GL). $K_{p,i}$ values at 37 °C were estimated. The 32 compounds were nicotine (in free-base form), seven toxicants (propanal, acetone, hydroxyacetone, benzene, toluene, *p*-xylene, and ethylbenzene), and 24 flavor chemicals (2,3-pentanedione ("acetyl propionyl"), isobutyl acetate, ethyl butyrate, butyl butyrate, isoamyl acetate, 2,3-dimethylpyrazine, 3-methyl-1-butanol, limonene, 2,3,5-trimethylpyrazine, *p*-cymene, benzaldehyde, (*Z*)-3-hexen-1-ol, menthol, 2-acetylpyrrole, benzyl alcohol, methyl salicylate, cinnamaldehyde, methyl anthranilate, (+)-aromadendrene, cinnamyl alcohol, methyl cinnamate, maltol, ethyl maltol, and coumarin). The measured log $K_{p,i}$ values were found to be generally correlated with literature values of log $p^o_{L,i}$; the scatter is caused by variation in ζ_i between ~1 and ~1000. K_p measurements were attempted, but values were not reported for acetaldehyde, 2,3-butanedione (diacetyl), vanillin, and ethyl vanillin. Acetaldehyde was found to form significant amounts of its cyclic trimer and cyclic tetramer; for diacetyl, the evidence suggested significant amounts of reaction products, possibly hemiketals and ketals with PG/GL, and for vanillin and ethyl vanillin, the K_p values are large and accordingly more difficult to measure. f_g values are calculated using a range of K_p and TPM values.

Gaphical Abstract

[*]**Corresponding Author** Phone: (503) 725-2844; pankowj@pdx.edu.

The authors declare no competing financial interest.

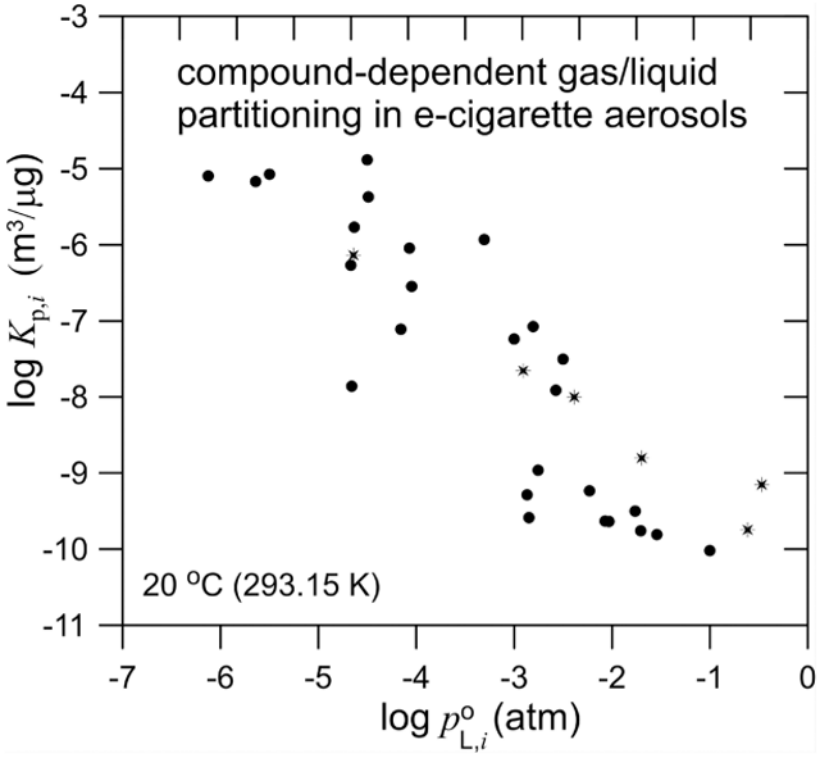

1. INTRODUCTION

Aerosols created by electronic cigarettes (e-cigarettes), conventional cigarettes, cigars, cannabis cigarettes, and “heat-not-burn” tobacco and cannabis products are all collections of small liquid droplets surrounded by a gas phase. Each chemical i in the aerosol (e.g., formaldehyde, acetaldehyde, acrolein, benzene, nicotine, etc.) that possesses some volatility (i.e., a nonzero vapor pressure) will partition between the gas and the droplet phases.[1] The compound-dependent equilibrium gas/particle coefficient $K_{p,i}$ ($m^3/\mu g$) is defined as[2]

$$K_{p,i}(\mathrm{m}^3/\mu\mathrm{g}) = \frac{c_{p,i}(\mu\mathrm{g}/\mu\mathrm{g})}{c_{g,i}(\mu\mathrm{g}/\mathrm{m}^3)} \quad (1)$$

where $c_{p,i}$ ($\mu g/\mu g$) is the concentration in the particle phase and $c_{g,i}$ ($\mu g/m^3$) is the concentration in the gas phase. Even under nonequilibrium conditions, the partition coefficient still plays a fundamental role as it determines the liquid- and air-side concentration gradients that drive mass transfer and equilibration (e.g., see Liss and Slater[3]). Here, we focus on $K_{p,i}$ values; their use in mass transfer calculations for inhaled aerosols that are highly physically dynamic (coagulation, deposition, etc.) is far beyond the scope of this work.

For gas/liquid partitioning[2]

$$K_{p,i}(\mathrm{m^3}/\mu\mathrm{g}) = \frac{RT}{10^6 \overline{\mathrm{MW}} \zeta_i p^{\circ}_{L,i}} \quad (2)$$

where R is the gas constant (8.2×10^{-5} m^3 atm mol^{-1} K^{-1}), T is temperature (K), $\overline{\mathrm{MW}}$ (g/mol) is the mol-average molecular weight of the absorbing liquid phase computed for a sample of that phase, namely [total g]/[total mols]), ζ_i (dimensionless, always > 0) is the mol-fraction-scale activity coefficient in the liquid (L) phase, and $p^{\circ}_{L,i}$ is the vapor pressure (atm) of pure liquid i at temperature T. For a compound that is a solid (when pure) at the temperature of interest, $p^{\circ}_{L,i}$ is the *subcooled* liquid vapor pressure of the pure compound, because in a liquid aerosol droplet, i is in a liquid state. $K_{p,i}$ values can be predicted using eq 2 with known/estimated values of $p^{\circ}_{L,i}$, ζ_i, and $\overline{\mathrm{MW}}$.[2] Time scales for reaching gas/liquid equilibrium in aerosols have been studied.[4]

$K_{p,i}$ values together with the total particulate matter (TPM, $\mu g/m^3$) concentration for the aerosol determine the equilibrium fraction of each compound i in the gas ($f_{g,i}$) and particle ($f_{p,i}$) phases,[1–5] which affect deposition in the respiratory tract (RT).[5] For the overall aerosol volume, assuming that the volume of the suspended TPM phase is negligible, then $c_{g,i}$ gives a good approximation of the gas-associated mass concentration ($\mu g/m^3$ of total aerosol). The mass concentration ($\mu g/m^3$ of total aerosol) in the TPM is $K_{p,i}$TPM. Thus, [1,2,5]

$$f_{g,i} = \frac{c_{g,i}}{c_{g,i} + c_{p,i}\mathrm{TPM}} = \frac{1}{1 + K_{p,i}\mathrm{TPM}} \quad (3)$$

$$f_{p,i} = \frac{c_{p,i}\mathrm{TPM}}{c_{g,i} + c_{p,i}\mathrm{TPM}} = \frac{K_{p,i}\mathrm{TPM}}{1 + K_{p,i}\mathrm{TPM}} \quad (4)$$

$$f_{g,i} + f_{p,i} = 1 \quad (5)$$

$$\frac{\text{mass in gas phase}}{\text{mass in PM}} = \frac{c_{g,i}}{c_{p,i}\mathrm{TPM}} = \frac{1}{K_{p,i}\mathrm{TPM}} \quad (6)$$

$$\frac{\text{mass in PM}}{\text{mass in gas phase}} = \frac{c_{p,i}\mathrm{TPM}}{c_{g,i}} = K_{p,i}\mathrm{TPM} \quad (7)$$

Being a pure-chemical physical property, $p^{o}_{L,i}$ is known for many compounds. Propylene glycol (PG) and glycerol (GL) are the dominant chemicals in the "e-liquids" used in electronic cigarettes and thus are the dominant chemicals in the aerosol droplets formed in the vaping process. ζ_i values in PG/GL mixtures are generally not known. The ζ_i can be near unity when i is polar, i.e., like PG and GL. For increasingly nonpolar i, ζ_i will become increasingly larger than 1. Regarding MW, the MW values for PG and GL are 76.09 and 92.09 g/mol, respectively; the densities at 20 °C are 1.04 and 1.26 g/mL, respectively. Thus, for an e-liquid that is 50/50 by volume PG/GL, then $\overline{MW} \approx 84\,g/mol$; for an e-liquid that is 50/50 by weight PG/GL, then $\overline{MW} = 83.3\,g/mol$. Nonzero concentrations of nicotine, flavor chemicals, other additives such as acids and water will all affect $\overline{MW}$. For a 50/50 by volume mixture of PG/GL that has been spiked with nicotine to a level of 24 mg/mL, then $\overline{MW} \approx 85\,g/mol$. For a 50/50 by volume mixture of PG/GL that has absorbed 10% by volume water (as from the laboratory environment or the interior of the RT), then $\overline{MW} \approx 64\,g/mol$; by itself, such a change will tend to increase K_p values by ~30% and will in most cases be counteracted by increases in ζ_i Here, we measured K_p values for 32 compounds as spiked into 50/50 by weight PG/GL with $\overline{MW}$ remaining at ~83.3 g/mol. The 32 compounds included nicotine, seven toxicant compounds, and 24 flavor chemicals. Though not studied directly here, PG, GL, and water will also follow eqs 1–7).

2. MATERIALS AND METHODS

Vapor Pressure.

Values of log $p^{o}_{L,i}$ at 20 and 37 °C (human body temperature) for 32 compounds studied here are given in Table 1. Twenty-four of the 32 compounds are liquids (L) at 20 °C; 28 are liquids at 37 °C. For those that are liquids at 20 °C and/or 37 °C (T = 293.15 and 310.15 K), log $p^{o}_{L,i}$ was based on published temperature-dependent functionalities. The same applies analogously to log $p^{o}_{S,i}$ for compounds that are solids (S) at 37 °C and/or 20 °C; to obtain $p^{o}_{L,i}$ at 37 and/or 20 °C, the enthalpy of fusion $\Delta H_{fus,i}$ (kJ/mol) was assumed constant in the application of[11]

$$\ln p^{o}_{L,i} = \ln p^{o}_{S,i} + \frac{\Delta H_{fus,i}}{RT_{m,i}}\left(\frac{T_{m,i}}{T} - 1\right) \quad (8)$$

where $T_{m,i}$ (K) = melting point of i at 1 atm (because of the general steepness of S/L phase boundaries in P vs T phase diagrams, $T_{m,i}$ is essentially the same as the triple point temperature) and R = 0.00831 kJ mol^{-1} K^{-1}. Because $\Delta H_{fus,i} > 0$, when $T < T_{nm,i}$ then $p^{o}_{L,i} > p^{o}_{S,i}$. The values of $\Delta H_{fus,i}$ used with eq 8 are given in Table 1.

$K_{p,i}$ Measurements.

The 32 compounds were divided into groups "1", "2", and "3" based on rough initial estimations of expected K_p (~low, ~medium, and ~high log K_p, respectively). Four

additional compounds were also studied, but the $K_{p,i}$ values are not reported because of complications due to (1) formation of a cyclic trimer and cyclic tetramer (acetaldehyde), (2) likely formation of hemiketals and ketals with PG/GL (diacetyl), and (3) low volatility (vanillin and ethyl vanillin). All measurements were carried out at 20 °C using 50/50 by weight mixtures of PG (MW = 76.09 g/mol) and GL (MW = 92.09 g/mol). Various standard stock mixtures (SSMs) were prepared as mixtures of initially pure (neat) compounds (no solvent was used) for spiking the PG/GL solution. For group 1, standard stock mixture 1 (SSM-1) was prepared; for group 2, standard stock mixture 2 (SSM- 2) was prepared. The concentrations in SSM-1 and SSM-2 ranged from 30 to 300 μg/μL. For measurement of the $K_{p,i}$ values for the 13 compounds in groups 1 and 2, 8 μL of SSM-1 and 50 μL of SSM-2 were spiked into each of three replicate 5 mL volumes of 50/50 by weight PG/GL in glass 155 mL crimp top (Teflon-faced septum) bottles. For each of the 13 compounds, the final solution-phase concentration was in the range 0.06–2.1 μg/μL; higher concentrations were used for compounds that were less volatile. Several minutes of inclined (~20°) rotation was used to mix the liquid followed by a 24 h headspace equilibration period. This was followed by sampling of 50 μL aliquots of headspace gas (5 replicates) with a 100 μL gastight syringe (Hamilton Company Inc., Reno, Nevada). Injection occurred into the injection port (235 °C, 1-to-5 split) of an Agilent 7890A gas chromatograph (GC, Santa Clara, CA). The GC was interfaced to an Agilent 5975C mass spectrometer (MS) operated in electron impact (70 eV) ionization mode. The fused silica capillary GC column was 30 m long with 0.25 mm i.d. and a 1.4 μm film thickness coating of Rxi-624Sil MS (Restek Inc., Bellefonte, PA). The GC temperature program was 40 °C for 3.5 min, ramp to 100 °C at 12 °C/min, ramp to 250 °C at 15 °C/min, hold at 250 °C for 1 min, and then 10 °C/min to 230 °C. For calibration, 50 μL volumes of gas standards of the 13 compounds were also analyzed by GC/MS. The standards were prepared by injecting 2–20 μL of SSM-1 and SSM-2 into a 2 L glass static dilution bottle (Kimble Chase, Vineland, NJ); the bottle was held at 40 °C for 30 min and then at 20 °C for 2 h; on the basis of prior experience with gas standards,[12] it was assumed that 100% of each of the 13 compounds evaporated to the gas phase in the bottle.

For the 19 compounds in group 3, a 50 μL headspace gas sample did not provide sufficient analyte: most of the group 3 compounds exhibit relatively large K_p values, making for relatively low c_g values (see eq 1). Two replicate 60 mL glass “VOA” vials (Thermo Scientific Inc., Texas) were charged with 25 mL of 50/50 PG/GL. For each replicate, 20–230 mg of each group 3 compound was then weighed into the PG/GL, giving final concentrations in the PG/GL between 0.78 and 9.23 μg/μL. The vials were sealed with 0.125 in. thick PTFE-faced silicone septa, stirred for ~30 min with a Teflon-coated stirbar, covered with aluminum foil, then equilibrated for 24 h. The headspace was then sampled at 10 mL/min as follows. The inlet end of a 10 cm length of 0.53 mm i.d. uncoated fused silica capillary tubing (Restek, Bellefonte, PA) passed through the septum and terminated in the headspace of the vial. The outlet end of the tubing was connected to an adsorption/thermal desorption (ATD) gas sampling cartridge (Camsco Inc., Houston, TX) packed with 100 mg of 35/60 mesh Tenax TA followed by 200 mg of 60/80 mesh Carbograph 1 TD. The sample flow was drawn by a syringe pump (Model NE-1010, New Era Pump Systems Inc., Farmingdale, NY) equipped with a customized 300 mL syringe. N_2 gas at 10 mL/min was allowed to enter the vial through the septum via a 30 cm length of 0.53 mm i.d. uncoated

fused silica capillary tubing (Restek, Bellefonte, PA) that ended below the level of the PG/GL, thereby creating very small bubbles of N_2. No evidence was observed in the data of errors due to any bubble-created aerosol droplets (i.e., no evidence of biased-low $K_{p,i}$ values). A tee valve positioned between the cartridge and the syringe pump was used to periodically exhaust gas from the syringe, allowing verification at that time of the sample volume. For each vial, an initial 200 mL of headspace was discarded and not sampled with an ATD cartridge. Three 200 mL samples were then obtained with three cartridges followed by five 100 mL samples obtained with five cartridges, which was then followed by five 50 mL replicates with five cartridges. (The range of sample volumes ensured that all compounds could be quantitated within reliable portions of their calibrations.) After sampling, a 5 min flow of N_2 at 40 mL/min was passed into the inlet end of each cartridge to remove oxygen. The cartridges were loaded into a TurboMatrix 650 ATD unit (PerkinElmer, Waltham, MA). Prior to desorption, the unit automatically loaded each cartridge with 24 ng of fluorobenzene as an internal standard. Each cartridge was thermally desorbed at 285 °C for 10 min (backflush direction) with the TurboMatrix 650 interfaced to the same GC column and GC/MS as described above. In the TurboMatrix 650, 40 mL/min of the desorption stream was focused on a Tenax-TA intermediate focusing trap (IFT) set at —10 °C. The remaining 25 mL/min was discarded as the “inlet split”. Upon completion of ATD cartridge desorption, the IFT was thermally desorbed at 295 °C for 4 min at 25 psi He pressure and a flow of ~24 mL/min with ~4 mL/min proceeding onto the column via a 225 °C transfer line (~20 mL/min was discarded by the TurboMatrix 650). Data acquisition began when the IFT desorption was started. The GC temperature program was 40 °C for 2 min, ramped to 100 °C at 10 °C/min, ramped to 280 °C at 12 °C/min, and then programmed to 230 °C at 10 °C/min. For multipoint calibration for each analyte, 4 μL aliquots of standards in isopropyl alcohol were spiked into the inlet ends of clean cartridges to obtain mass amounts of 2–1400 ng per analyte; the final concentrations in the PG/GL solution were verified by taking aliquots of 25, 50, and 100 μL, diluting in isopropyl alcohol, and analyzing by GC/MS.

Replicate blank cartridges were prepared using gas sample volumes of 200 mL drawn through the experimental setup with no PG/GL solution as yet placed in the vial.

An additional series of measurements was carried out with nicotine alone using the experimental setup for group 3 compounds. The series was conducted to ensure that the K_p value reported is that for free-base nicotine ($K_{p,fb}$), i.e., unaffected by any significant degree of protonation. (Protonation will greatly alter the aerosol K_p value for total nicotine according to[5,13,14] $K_p = K_{p,fb}/\alpha_{fb}$, where α_{fb} is the fraction of the nicotine in the particle phase that is in the free-base form; values of α_{fb} for selected e-liquids were reported by Duell et al.[15])

Here, 25 mL of 50/50 (by weight) PG/GL was spiked with 103 mg of nicotine to give a level of 4.12 μg/μL. Fifteen milliliters of ammonia gas was then bubbled into the solution (1/1 nicotine/ammonia mol ratio). A small stir bar mixed the solution for 24 h. Sampling of the headspace with bubbling of the PG/GL liquid proceeded as above. Eight ATD cartridge samples were collected and analyzed as above: four replicates at 200 mL and four replicates at 100 mL.

3. RESULTS

The log $K_{p,i}$ values measured at 20 °C are given in Table 1. Also given are the corresponding values of ζ_i at 20 °C calculated using eq 2 with the log $p^o_{L,i}$ values given and with $\overline{MW}$ = 83.3 g / mol for 50/50 PG/GL. The accuracies of the calculated ζ_i values are subject to errors in the log $p^o_{L,i}$. Furthermore, as noted above for acetaldehyde and diacetyl, aldehyde and ketone compounds are subject to reactions at the carbonyl group: detailed studies as to whether any of the aldehyde and ketone compounds in Table 1 (marked with *) were affected by such reactions were not carried out here. Any such effect would cause the reported K_p value to be somewhat too high. Overall, the K_p values for the compounds without an * are considered most reliable.

As noted elsewhere,[10] from eq 2, assuming that ζ_i is approximately independent of temperature,

$$K_{p,i}(310.15\text{K}) = \left[\frac{p^o_{L,i}(293.15)}{p^o_{L,i}(310.15)} \times \frac{310.15}{293.15}\right] \times K_{p,i}(293.15\text{K}) \quad (9)$$

$$\text{If} \quad \tau_{20\rightarrow 37} \equiv \left[\frac{p^o_{L,i}(293.15)}{p^o_{L,i}(310.15)} \times \frac{310.15}{293.15}\right] \quad (10)$$

$$K_{p,i}(310.15\text{K}) = \tau_{20\rightarrow 37} K_{p,i}(293.15\text{K}) \quad (11)$$

Values of log $K_{p,i}$, at 37 °C (normal human body temperature) calculated by eq 7 are given in Table 1. The average value of $\tau_{20\rightarrow 37}$ for the Table 1 compounds is 0.32, so on average in 50/50 PG/GL, the values of $K_{p,i}$ were found to decrease by a factor of ~3 as temperature increases from 20 to 37 °C.

Figure 1 is a plot for the measured log $K_{p,i}$ values vs log $p^o_{L,i}$ at 20 °C. Dashed lines are included for ζ = 1, 10, 100, and 1000 with $\overline{MW}$ = 83.3 g / mol. Because PG and GL are polar solvents, the points for the most polar molecules plot near the ζ = 1 line (propanal, acetone, and nicotine). For the molecules that are increasingly hydrophobic, the calculated ζ_i values increase. For comparisons with ζ values found in the literature for solutes in glycol-type solvents, for benzene at 25 °C Opris[16] measured ζ = 14.0 in 1,3-propanediol (an isomer of PG) and ζ = 44.2 in ethylene glycol (EG) (both EG and GL have one −OH group per carbon). The average is ζ = (14.2 + 44.2)/2 = 29. Here, for benzene in 50/50 PG/GL, we obtained ζ = 30 at 20 °C. Similar general agreement is shown in Table 2 for toluene and ethylbenzene. For larger nonpolar compounds such as limonene, *p*-cymene, and aromadendrene in 50/50 PG/GL, we found ζ = 780, 410, and 960, respectively.

In log $K_{p,i}$ vs log $p^{o}_{L,i}$ plots, it is well-known that data points for structurally related compounds are in general much more highly correlated than observed for a larger, multicompound-class data set as with alkanes and polycylic aromatic hydrocarbons (PAHs) partitioning to tobacco smoke PM.[17] This type of result is observed in Figure 1, wherein the points for *p*-cymene, limonene, *p*-xylene, ethylbenzene, toluene, and benzene exhibt their own mini correlation line.

4. DISCUSSION AND CONCLUSIONS

Within the $K_{p,i}$ expression, ζ_i occurs with $p^{o}_{L,i}$ as the product $\zeta_i p^{o}_{L,i}$. Assuming all $\zeta_i = 1$, Pankow[1] provided a plot of log $f_{g,i}$ vs log $p^{o}_{L,i}$ with lines for various TPM values between 10^7 and 10^9 μg/m^3. Here, because we have now obtained information regarding ζ_i values for compounds of interest in PG/GL, Figure 2 gives curves (at equilibrium) at 37 °C for log $f_{g,i}$ vs log($\zeta_i p^{o}_{L,i}$) with values for selected compounds of the latter marked on the upper *x*-axis. At equilibrium, for benzene, toluene, and limonene, 90% or more of the compounds will be in the gas phase even at TPM = 10^9 μg/m^3. For cinnamyl alcohol, maltol, and free-base nicotine, at equilibrium, 90% or more of the compounds will be in the particle phase even at TPM = 10^7 μg/m^3. Upon inhalation, deposition of particles and gaseous compounds will begin. For a gas/particle system initially at equilibrium, the deposition of a compound as a gas will move the system away from equilibrium and moreover enhance further volatilization from the inhaled particles that remain suspended. For compounds with even modest volatility, as perhaps with $K_p < 10^{-9}$ μg/m^3, a significant fraction of the overall gas + particle inhaled amount may deposit to respiratory tract surfaces even when particle deposition is inefficient.[5] The $K_{p,i}$ values obtained here will be useful in aerosol inhalation/deposition modeling efforts that seek to address such deposition questions: even when bulk gas/bulk liquid equilibrium is not present, they can be used to describe conditions directly at the gas/particle interface where the nonequilbrium mass transfer is occurring.

Acknowledgments

Funding

This work was supported by the U.S. National Institutes of Health, grant R01ES025257. Research reported was supported by the NIEHS and FDA Center for Tobacco Products (CTP). The content is solely the responsibility of the authors and does not necessarily represent the views of the NIH or the FDA.

ABBREVIATIONS

ATD	adsorption/thermal desorption
e-cigarette	electronic cigarette
e-liquid	electronic cigarette liquid
fb	free base
GC	gas chromatograph/chromatography

EG	ethylene glycol
GL	glycerol
IFT	intermediate focusing trap
PD	1,3-propanediol
PG	propylene glycol
SSM	standard stock mixture
TPM	total particulate matter
MS	mass spectrometer/spectrometry
MW	molecular weight
VOA	volatile organics analysis
w/w	weight/weight

REFERENCES

(1). Pankow JF (2017) Calculating compound dependent gas-droplet distributions in aerosols of propylene glycol and glycerol from electronic cigarettes. J. Aerosol Sci 107, 9–13.

(2). Pankow JF (1994) An absorption model of gas/particle partitioning in the atmosphere. Atmos. Environ 28, 185–188.

(3). Liss PS, and Slater PG (1974) Flux of gases across the air-sea interface. Nature 247, 181–184.

(4). Saleh R, Donahue NM, and Robinson AL (2013) Time scales for gas-particle partitioning equilibration of secondary organic aerosol formed from alpha-pinene ozonolysis. Environ. Sci. Technol 47, 5588–5594. [PubMed: 23647198]

(5). Pankow JF (2001) A consideration of the role of gas/particle partitioning in the deposition of nicotine and other tobacco smoke compounds in the respiratory tract. Chem. Res. Toxicol 14, 1465–1481. [PubMed: 11712903]

(6). Diaz MAE, Guetachew T, Landy P, and Voilley JA (1999) Experimental and estimated saturated vapour pressures of aroma compounds. Fluid Phase Equilib. 157, 257–270.

(7). Towler G, and Sinnott R (2012) Principles, Practice and Economics of Plant Process and Design; Butterworth-Heinemann, Oxford, 1320 p. Appendix C, https://booksite.elsevier.com/9780080966595/content/Appendices/Appendix%20C.pdf (accessed June 29, 2018).

(8). Soni M, Ramjugernath D, and Raal JD (2008) Vapor–liquid equilibrium for binary systems of 2,3-pentanedione with diacetyl and acetone. J. Chem. Eng. Data 53, 745–749.

(9). Petitjean M, Reyès-Pérez E, Pérez D, Mirabel Ph., and Le Calvé S (2010) Vapor pressure measurements of hydroxyacetalde-hyde and hydroxyacetone in the temperature range (273 to 356) K. J. Chem. Eng. Data 55, 852–855.

(10). Pankow JF, Luo W, Tavakoli AD, Chen C, and Isabelle LM (2004) Delivery levels and behavior of 1,3-butadiene, acrylonitrile, benzene, and other toxic volatile organic compounds in mainstream tobacco smoke from two brands of commercial cigarettes. Chem. Res. Toxicol 17, 805–813. [PubMed: 15206901]

(11). Prausnitz JM, Lichtenhaler RN, and de Azevedo EG Molecular Thermodynamics of Fluid-phase Equilibria, 860 pages. Eqs 11–13, p 640 Prentice-Hall Inc.: NJ, 1999.

(12). Pankow JF, Luo W, Isabelle LM, Bender DA, and Baker RJ (1998) Determination of a wide range of volatile organic compounds in ambient air using multisorbent adsorption/thermal desorption and gas chromatography/mass spectrometry. Anal. Chem 70, 5213–5221.

(13). Pankow JF, Mader BT, Isabelle LM, Luo W, Pavlick A, and Liang C (1997) Conversion of nicotine in tobacco smoke to its volatile and available free-base form through the action of gaseous ammonia. Environ. Sci. Technol. 31, 2428–2433.See also Errata, Environ. Sci. Technol 33, 1320.

(14). Pankow JF, Tavakoli AD, Luo W, and Isabelle LM (2003) Percent free-base nicotine in the tobacco smoke particulate matter of selected commercial and reference cigarettes. Chem. Res. Toxicol 16, 1014–1018. [PubMed: 12924929]

(15). Duell AK, Pankow JF, and Peyton DH (2018) Free-base nicotine determination in electronic cigarette liquids by 1H NMR spectroscopy. Chem. Res. Toxicol. 31, 431–434. [PubMed: 29775302]

(16). Opris I (1981) Determination and interpretation of activity-coefficients at infinite dilution of some hydrocarbons in terminal dihydroxy alcohols. Revista de Chimie (Bucharest) 32, 234–238.

(17). Liang C, and Pankow JF (1996) Gas/particle partitioning of organic compounds to environmental tobacco smoke: partition coefficient measurements by desorption and comparison to urban particulate material. Environ. Sci. Technol. 30, 2800–2805.

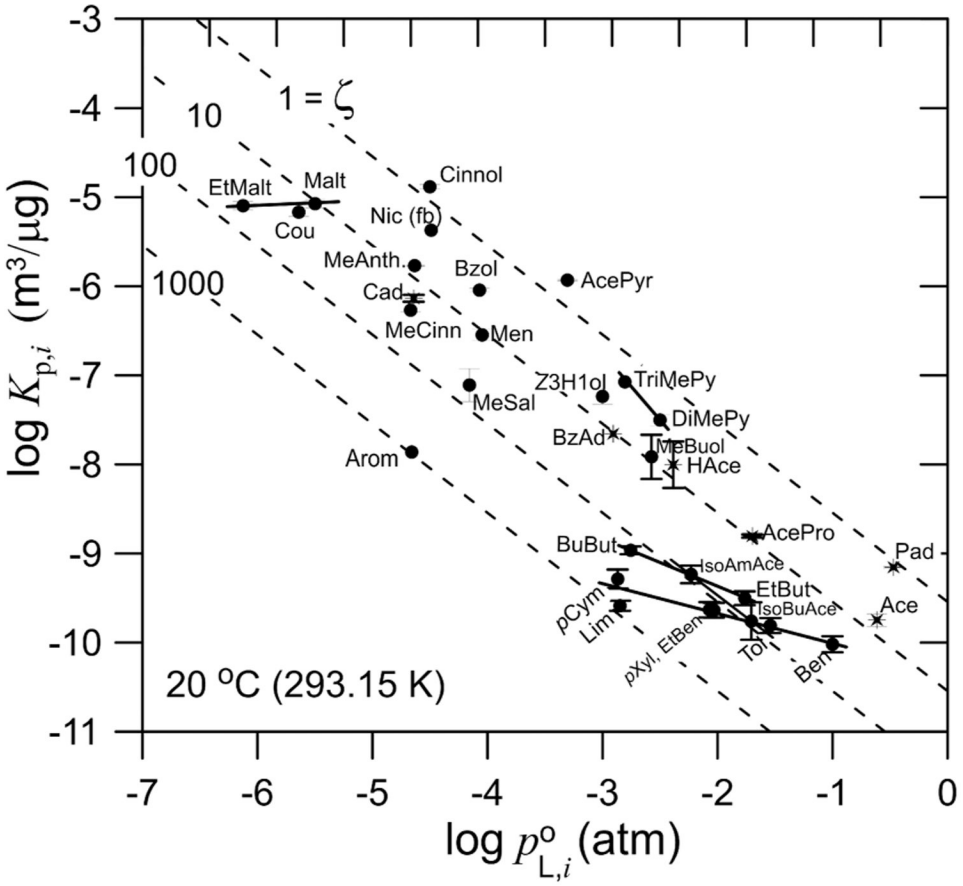

Figure 1.

Log K_p vs log p^o_L at 20 °C for 32 compounds partitioning to 50/50 (w/w) propylene glycol/glycerol (PG/GL). Mini correlation lines shown for related compounds. * for aldehydes and ketones; ● for all other compounds.

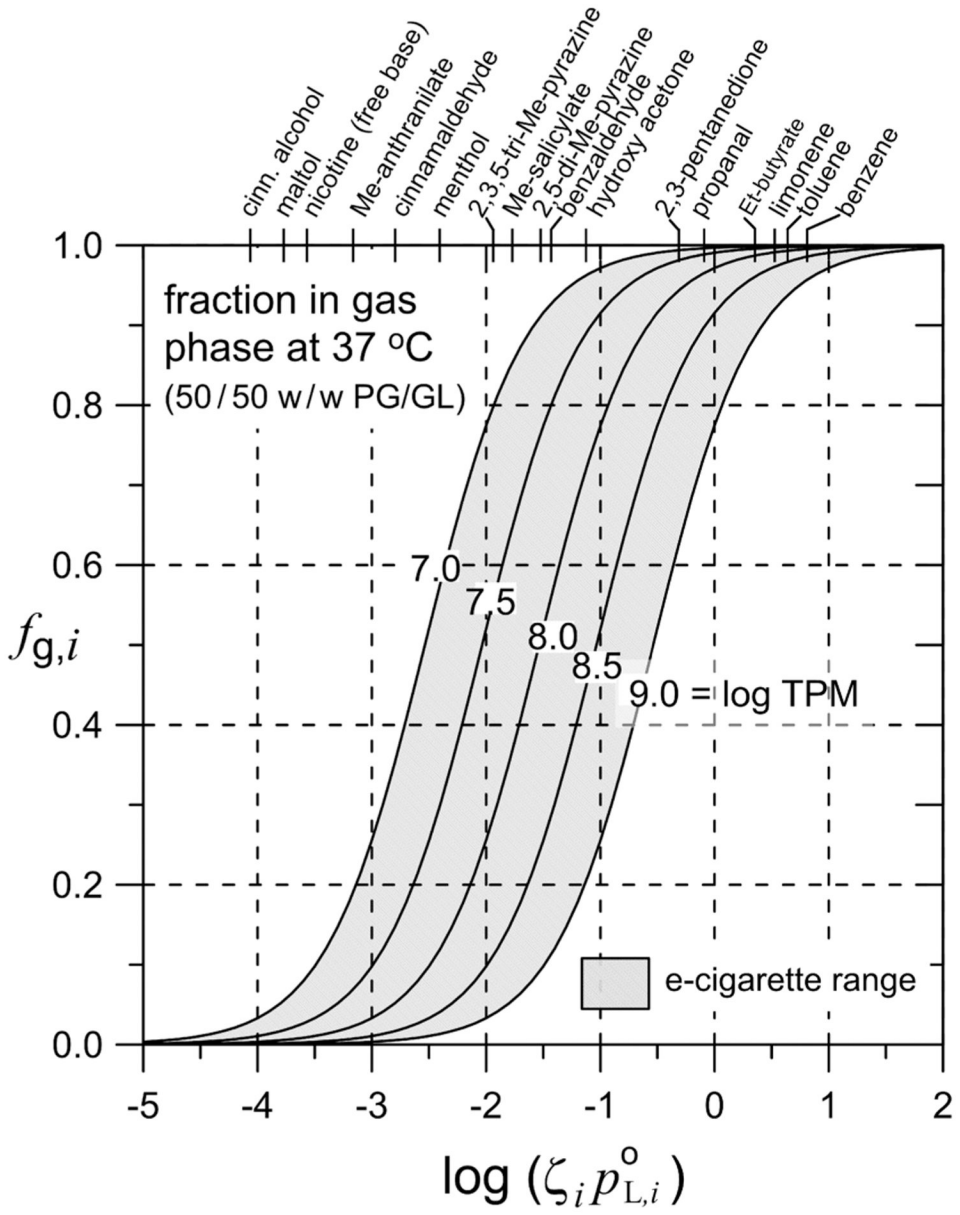

Figure 2.

$f_{g,i}$ vs log[$\zeta_i p^o_{L,i}$] at 37 °C for partitioning to 50/50 (w/w) propylene glycol/glycerol PG/GL) and a range of TPM (μg/m^3) values.

Chem Res Toxicol. Author manuscript; available in PMC 2019 May 13.

Table 1.

Log K_p and Related Values for 32 Compounds[a]

compound	group	abbr.	melting point (°C)	log p_L^o at 20 °C (atm)	log K_p (av, N = 3)[b] ($m^3/\mu g$, 20 °C) (measured)	SD of log K_p (N = 3)[b] ($m^3/\mu g$, 20 °C) (measured)	ζ (20 °C)	log p_L^o at 37 °C (atm)[a]	log [ζ p_L^o] at 37 °C	$\tau_{20\rightarrow37}$	log K_p($m^3/\mu g$, 37 °C) (extrapolated)
benzene	1	Ben	5.5	−1.00[c]	−10.02	0.09	30	−0.67	0.81	0.49	−10.32
toluene	1	Tol	−95	−1.54[c]	−9.81	0.08	65	−1.17	0.64	0.45	−10.15
isobutyl acetate	1	IsoBAc	−99	−1.71[c]	−9.76	0.21	84	−1.32	0.60	0.44	−10.12
acetone*	1	Act	−95	−0.61[c]	−9.75	0.07	6.6	−0.31	0.52	0.52	−10.03
ethylbenzene	1	EtBen	−95	−2.03[c]	−9.64	0.08	130	−1.62	0.51	0.41	−10.03
p-xylene	1	pXyl	13	−2.07[c]	−9.63	0.09	150	−1.65	0.51	0.40	−10.03
limonene	1	Lim	−74	−2.85[d]	−9.59	0.06	780	−2.37	0.53	0.35	−10.04
ethyl butyrate	1	EtBut	−93	−1.76[c]	−9.50	0.08	53	−1.37	0.35	0.43	−9.87
p-cymene	1	pCym	−68	−2.87[c]	−9.29	0.11	410	−2.38	0.24	0.34	−9.75
isoamyl acetate	3	IsoAmAc	−78	−2.23[c]	−9.23	0.10	84	−1.79	0.14	0.38	−9.65
propanal*	2	Pad	−81	−0.47[e]	−9.15	0.01	1.2	−0.17	−0.09	0.54	−9.43
butyl butyrate	1	BuBut	−92	−2.76[f]	−8.96	0.04	150	−2.32	−0.14	0.39	−9.37
2,3-pentanedione*	2	AcPr	−52	−1.70[g]	−8.80	0.02	9.2	−1.27	−0.31	0.40	−9.20
hydroxyacetone*	1	Hact	−17	−2.38[h]	−8.00	0.26	7.0	−1.97	−1.13	0.41	−8.39
3-methyl-1-butanol	3	MeBuol	−117	−2.58[e]	−7.91	0.25	8.9	−2.00	−1.05	0.28	−8.46
(+)-aromadendrene	3	Arom	6.8	−4.66[i]	−7.86	NA	960	−4.20	−1.22	0.37	−8.30
benzaldehyde*	3	Bzad	−26	−2.91[c]	−7.66	NA	11	−2.45	−1.43	0.37	−8.08
2,3-dimethylpyrazine	3	DiMePy	12	−2.50[j]	−7.50	0.06	2.9	−1.99	−1.52	0.32	−7.99
(*Z*)-3-hexen-1-ol	3	Z3H1ol	−61	−3.00[k]	−7.23	0.09	5.0	−2.56	−1.86	0.38	−7.66

compound	group	abbr.	melting point (°C)	log p_L^o at 20 °C (atm)	log K_p (av, N = 3)[b] ($m^3/\mu g$, 20 °C) (measured)	SD of log K_p (N = 3)[b] ($m^3/\mu g$, 20 °C) (measured)	ζ (20 °C)	log p_L^o at 37 °C (atm)[a]	log [ζ p_L^o] at 37 °C	$\tau_{20\rightarrow37}$	log K_p($m^3/\mu g$, 37 °C) (extrapolated)
methyl salicylate	3	MeSal	−7.5	−4.16[c]	−7.11	0.19	53	−3.50	−1.77	0.23	−7.74
2,3,5-trimethylpyrazine	3	TriMePy	<−10	−2.81[j]	−7.07	NA	2.2	−2.28	−1.94	0.31	−7.58
menthol	3	Men	37	−4.05[c]	−6.55	0.07	11	−3.46	−2.41	0.27	−7.11
methyl cinnamate	3	MeCinn	36	−4.67[c]	−6.27	0.02	25	−4.06	−2.66	0.26	−6.86
cinnamaldehyde*	3	Cad	−7.5	−4.64[c]	−6.14	0.04	17	−4.04	−2.80	0.26	−6.72
benzyl alcohol	3	Bzol	−15	−4.07[c]	−6.04	0.02	3.8	−3.41	−2.84	0.23	−6.68
2-acetylpyrrole	3	AcPyr	~90	−3.31[l]	−5.93	0.01	0.50	−2.65	−2.95	0.23	−6.56
methyl anthranilate	3	MeAnth	24	−4.63[c]	−5.77	0.01	7.3	−4.03	−3.16	0.26	−6.35
nicotine	3	Nic	−79	−4.49[m]	−5.37 (=$K_{p,fb}$)	NA	2.1	−3.89	−3.57	0.27	−5.95 (=$K_{p,fb}$)
coumarin	3	Cou	71	−5.64[l]	−5.17	0.05	19	−4.99	−3.72	0.23	−5.80
ethyl maltol	3	EtMalt	~87	−6.13[l]	−5.10	0.05	48	−5.43	−3.75	0.21	−5.77
maltol	3	Malt	162	−5.50[l]	−5.07	0.04	11	−4.80	−3.77	0.21	−5.75
cinnamyl alcohol	3	Cinnol	33	−4.50[c]	−4.88	0.02	0.70	−3.91	−4.07 av:	0.27 0.34	−5.45

[a] For aldehydes and ketones (marked with *), log K_p values may be too large by ~0.1 due to artifacts caused by polymerization, hemiacetal formation, acetal formation, hemiketal formation, and/or ketal formation in the PG/GL liquid phase; log K_p ($m^3/\mu g$) values were measured at 20 °C in 50/50 (by weight) propylene glycol/glycerol. Corresponding activity coefficient values ζ were calculated by eq 2 using p_L^o at 20 °C and $\overline{MW} = 83.3\ g\ /\ mol$. Values of p_L^o at 20 and 37 °C were used to obtain K_p values extrapolated to 37 °C by eq 9.

[b] N = 3 unless NA (not available)is given for the standard deviation for the measured log K_p at 20 °C, in which case N = 1.

[c] Antoine eq as given at https://webbook.nist.gov (accessed June 29, 2018).

[d] Antoine eq from Diaz et al.[6]

[e] Antoine eq as given in Towler and Sinnott.[7]

[f] p_L^o at 25 °C from http://www.thegoodscentscompany.com corrected to 20 °C using ΔH_{vap} for other butyrates.

[g] Antoine eq for p_L^o as given in Soni et al.[8]

[h] Antoine eq for p_L^o as given in Petitjeanet al.[9]

[i] p_L^o at 25 °C from http://www.thegoodscentscompany.com (accessed June 29, 2018). p_L^o at 20 °C calculated using ΔH_{vap} from https://www.chemeo.com/cid/10-581-5/Aromadendrene.pdf (accessed June 29, 2018).

[j] p_L^o at 25 °C from http://www.thegoodscentscompany.com (accessed June 29, 2018). p_L^o at 20 °C calculated using ΔH_{vap} from https://webbook.nist.gov (accessed June 29, 2018).

[k] p_L^o at 25 °C from http://www.thegoodscentscompany.com/, accessed June 29, 2018. p_L^o at 20 °C calculated using ΔH_{vap} from https://www.chemeo.com/cid/18-655-5/3-Hexen-1-ol,%20(Z)-.pdf, accessed June 29, 2018.

[l] p_L^o at 25 °C from Pubchem, Open Chemistry Database, https://pubchem.ncbi.nlm.nih.gov/, accessed June 29, 2018. p_L^o calculated using eq 8 with ΔH_{fus} (kJ/mol) as follows: 2-Acetylpyrrole, 14.08; coumarin, 19.14 kJ/mol; vanillin, 22.40 kJ/mol; ethyl vanillin, 23.10 kJ/mol, all from https://webbook.nist.gov, accessed June 29, 2018. Experimental ΔH_{fus} values were not found for maltol and ethyl maltol, so ΔH_{fus} = 19.68 kJ/mol was used for both.

[m] Pankow.[10]

Table 2.

Comparison of ζ Values for Benzene, Toluene, and Ethyl Benzene as Obtained by Opris[16] and in This Work

	Opris[16] at 25 °C			this work at 20 °C
compound	**ζ in 1,3-PD[a]**	**ζ in EG[b]**	**ζ average**	**ζ in 50/50 PG[c]/GL[d]**
benzene	14.0	44.2	29	30
toluene	23.5	82.1	53	65
ethylbenzene	36.2	141	89	130

[a] 1,3-PD = 1,3-propanediol.

[b] EG = ethylene glycol.

[c] PG = propylene glycol.

[d] GL = glycerol.